

Copyright © 2012 IEEE

*Reprinted from
IEEE Microwave and wireless components letters, Vol. 22, Issue 8, 2012*

Personal use of this material is permitted. Permission from IEEE must be obtained for all other uses, in any current or future media, including reprinting/republishing this material for advertising or promotional purposes, creating new collective works, for resale or redistribution to servers or lists, or reuse of any copyrighted component of this work in other works.

A 60 to 77 GHz Switchable LNA in an RF-MEMS Embedded BiCMOS Technology

Ahmet Çağrı Ulusoy, *Student Member, IEEE*, Mehmet Kaynak, *Student Member, IEEE*, Tatyana Purtova, *Member, IEEE*, Bernd Tillack, and Hermann Schumacher, *Member, IEEE*

Abstract—In this letter, a 60 to 77 GHz switchable low-noise amplifier is presented. The IC is realized in a radio frequency microelectromechanical systems embedded $0.25\ \mu\text{m}$ SiGe-C BiCMOS technology. Measured results show that the presented IC achieves good performance in both frequency bands in terms of gain, noise figure and power consumption. These results demonstrate the successful monolithic integration of RF-MEMS switches with active devices, and a first time implementation of a reconfigurable low noise amplifier at such high frequencies.

Index Terms—BiCMOS integrated circuits (ICs), dual band, low-noise amplifiers (LNAs), millimeter wave integrated circuits, MMICs, radio frequency microelectromechanical systems (RF-MEMS), switches, tunable circuits and devices.

I. INTRODUCTION

RADIO frequency microelectromechanical systems (RF-MEMS) are an interesting research topic, as RF-MEMS components increasingly find applications in several areas at X-band to millimeter-wave frequencies [1]. In general, integration of RF-MEMS components in electronics is a major problem in terms of cost and addition of interconnect parasitics. This limits the range of potential applications, especially for higher frequencies. In that sense, cofabrication of RF-MEMS and electronic devices would be very advantageous [2], and such integration potentially would open up more application windows for RF-MEMS. One example of such integration can be found in [3], where an X-band, dual-path power amplifier is presented, which utilizes RF-MEMS switches that are fabricated on the same GaAs substrate.

In this work, a reconfigurable LNA in a back end of line (BEOL) embedded RF-MEMS technology is presented. Using the same technology, a 3 to 4 GHz switchable voltage controlled oscillator has already been presented in [4], and this work extends the applicability to millimeter-wave frequencies, by presenting novel results of a 60 to 77 GHz switchable LNA.

Manuscript received February 22, 2012; revised April 17, 2012; accepted June 18, 2012. Date of publication July 10, 2012; date of current version August 03, 2012. This work was supported in part by the European Commission through the FP7 project FLEXWIN.

A. C. Ulusoy, T. Purtova, and H. Schumacher are with the Institute of Electron Devices and Circuits, Ulm University, Ulm D-89081, Germany (e-mail: ahmet.ulusoy@uni-ulm.de).

M. Kaynak is with the IHP, Frankfurt D-15236, Germany (e-mail: kaynak@ihp-microelectronics.com).

B. Tillack is with the IHP, Frankfurt D-15236, Germany and also with Technische Universität Berlin, Berlin D-10623, Germany.

Color versions of one or more of the figures in this paper are available online at <http://ieeexplore.ieee.org>.

Digital Object Identifier 10.1109/LMWC.2012.2205562

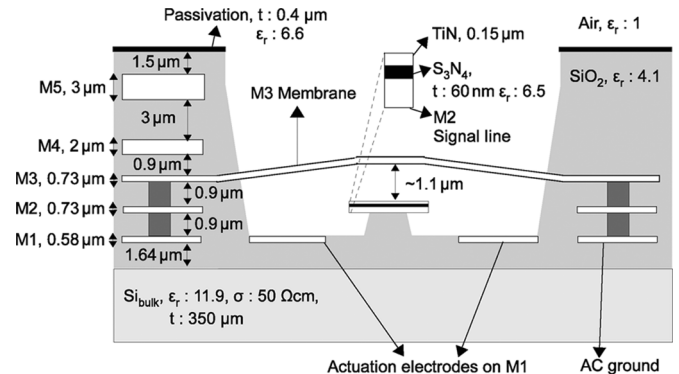


Fig. 1. Cross section of the BEOL embedded RF-MEMS shunt capacitive switch. M1–5 depict the metal layers of the core technology, while the switch is realized between M1 to M3 layers.

II. TECHNOLOGY

In Fig. 1 the cross section of the RF-MEMS switch is displayed. The core technology is the IHP SG25H1 $0.25\ \mu\text{m}$ SiGe-C BiCMOS with five metal layers (M1–5). The switch consists of an M3 membrane, an M2 signal line and the actuation electrodes on M1. It is realized by the removal of the SiO_2 in the switch area by wet etching, which adds only one additional mask layer to the standard technology process. The released M3 membrane bends upward due to residual mechanical stress, which is optimized by rigorous mechanical simulations and process optimization [4]. When an actuation voltage is applied on the M1 electrodes, the membrane is pulled down making contact with the TiN layer above the M2 signal line. The TiN layer and the dielectric layer underneath is technology standard for MIM capacitors. This mechanical movement results in a high or low capacitance between the membrane and the signal line for the down or up positions of the membrane, respectively. Typical actuation voltage is in the range of 20–25 V, while for reliable operation 40 V is recommended. The switching time is around 4 to 5 μs .

In Fig. 2, the top view and the dimensions of the membrane and the signal line are displayed. The membrane has four supporting beams which are connected to the ac ground of the circuit. For electrical modeling, the signal line and the membrane are EM-simulated in ADS Momentum, while the switch capacitance is included as a lumped component between the two structures. The value of the switch capacitance is extracted from CV measurements, and equals 22 fF for the up-state, and 220 fF for the down-state.

In Fig. 3, the simulated performance of the switch is displayed for the up- and down-states. The simulations show an insertion loss less than 1 dB up to 100 GHz, and an isolation better than

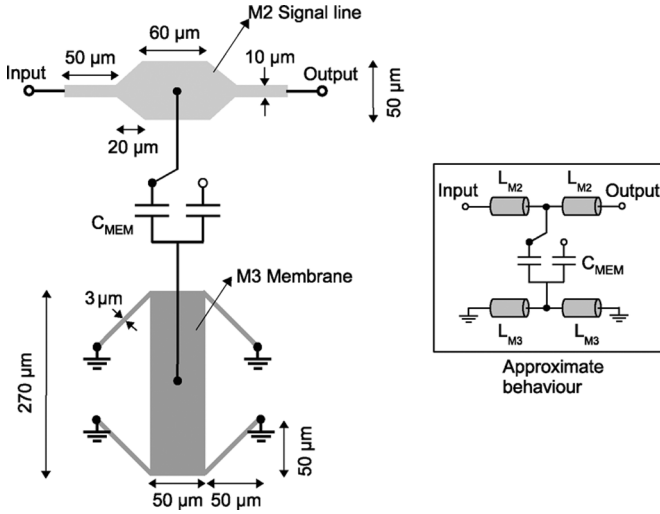


Fig. 2. EM-simulation based model of the shunt capacitive RF-MEMS switch used in circuit simulations. $C_{MEM} = 220$ fF (down state), 22 fF (up state). The capacitance area equals $50 \times 50 \mu\text{m}^2$.

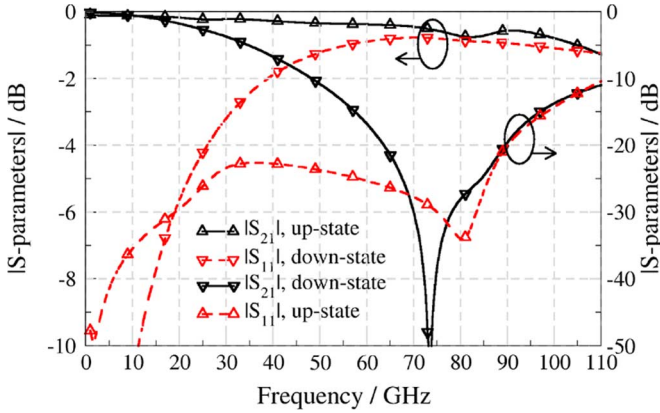


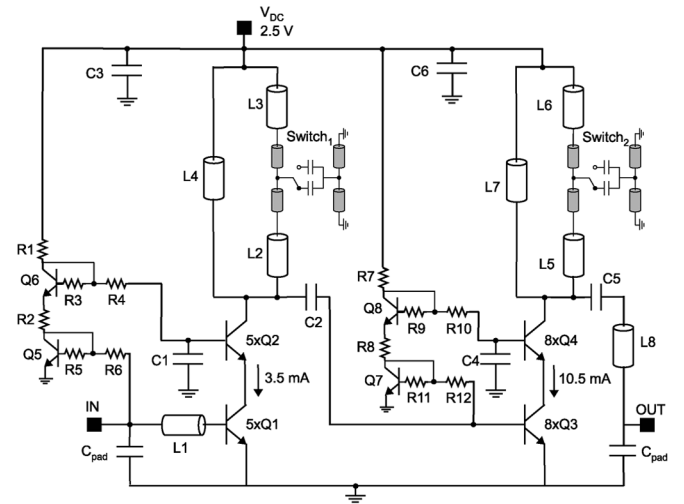
Fig. 3. Simulated switch performance for the up- and down-states of the membrane.

15 dB from 58 to 96 GHz. The isolation is defined by the ratio of $|S_{21}|$ for the up- and down-states of the switch.

III. CIRCUIT DESIGN

The schematic of the 60/77 GHz switchable LNA is shown in Fig. 4. The LNA consists of two stages of cascode amplifiers. The inductors L_{1-8} are realized as thin-film-microstrip lines between M5 and M1. Considering the approximate behavior of the RF-MEMS switches shown in Fig. 2, the most convenient way to integrate the switch into the design is including it as part of a reconfigurable transmission line. This is done here for the loads of the two stages L_2/L_3 and L_5/L_6 , respectively. These realize tapped inductors in combination with the RF-MEMS switches, where the tap can be shorted to ground by the switch capacitance. If we consider the first stage, when the RF-MEMS switch is in the up-state the total load inductance approximately equals L_4 parallels $(L_2 + L_3)$, while in the down state the total inductance becomes approximately L_4 parallels L_2 . By this means, the switchable dual-band operation in the desired frequency bands is achieved by properly adjusting the line lengths of L_{2-7} .

A reconfigurable input matching network was not needed, as the two bands of operation are relatively close to each other.



L1,2,3,5,6,8	L4,7	C1,4	C2,5	C3,6	C_{pad}	R1	R2	R3,5,9,11	R4,6,10,12	R7	R8
l:150 μm w:4 μm 0.08 nH (Q:14)	l:220 μm w:4 μm 0.12 nH (Q:12)	2 pF	40 fF	5 pF	20 fF	0.55 k Ω	0.38 k Ω	5 k Ω	1 k Ω	0.27 k Ω	0.1 k Ω

Fig. 4. Schematic of the 60–77 GHz dual-band reconfigurable LNA. The transistor dimensions are $N \times 0.21 \times 0.84 \mu\text{m}^2$, where N is the number of emitter fingers.

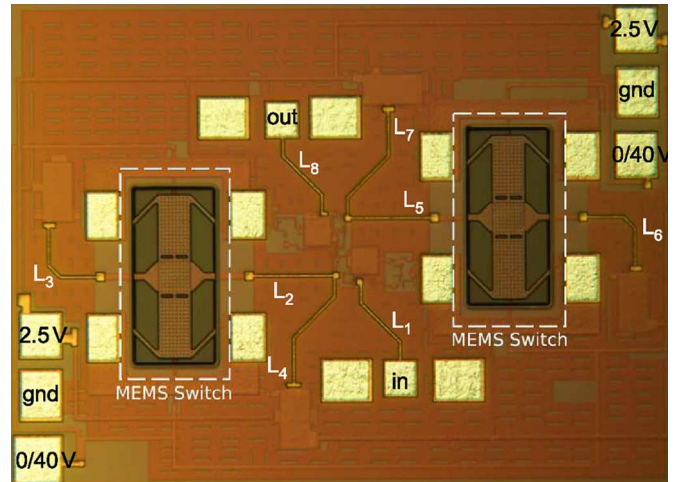


Fig. 5. Chip photograph of the 60/77 GHz switchable LNA. The total IC area is $0.75 \times 1.05 \text{ mm}^2$.

Instead, the transistors Q_1 and Q_2 are properly scaled to enable good noise and power match at both 60 and 77 GHz. The second stage transistors Q_3 and Q_4 are chosen to be larger with eight emitter fingers and are biased at 10.5 mA current providing higher total gain, while Q_1 and Q_2 have five emitter fingers and are biased at 3.5 mA collector current, providing lower noise figure (NF). The five finger devices in common-emitter configuration exhibit a simulated minimum noise figure (NF_{min}) of 4.4 dB at 60 GHz, and 5.4 dB at 77 GHz.

IV. EXPERIMENTAL RESULTS

The chip photograph of the realized 60/77 GHz switchable LNA is displayed in Fig. 5. The total chip area, including measurement pads is $0.75 \times 1.05 \text{ mm}^2$, and the IC consumes a total of 16 mA from a 2.5 V dc voltage source.

In Fig. 6, the measured S-parameters and NF of the designed 60/77 GHz switchable LNA are given for the up-state of the

TABLE I
SUMMARY OF THE RESULTS

	Technology	f_T/f_{max} (GHz)	Gain (dB)	3-dB BW (GHz)	NF (dB)	P_{DC} (mW)	FOM (mw^{-1}) *
up-state	0.25 μm BiCMOS	190/220	18.7 to 21	51-60 ⁺	6.8 to 7.3	40	0.55 ⁺
down-state	0.25 μm BiCMOS	190/220	21.3 to 23	66-78 ⁺	7.6 to 8.4	40	0.78 ⁺
[5]	0.25 μm BiCMOS	200/200	18	60-64 [†]	6.5	27	0.67
[6]	0.18 μm BiCMOS	200/200	14.5	69-84	6.9	37	0.19
[7]	0.12 μm BiCMOS	200/290	14.7	56-70 [†]	4.5	10.8	1.5

* $\text{FOM} = \frac{\text{Gain}}{(NF-1) \cdot P_{DC}}$ + in average † graphically estimated

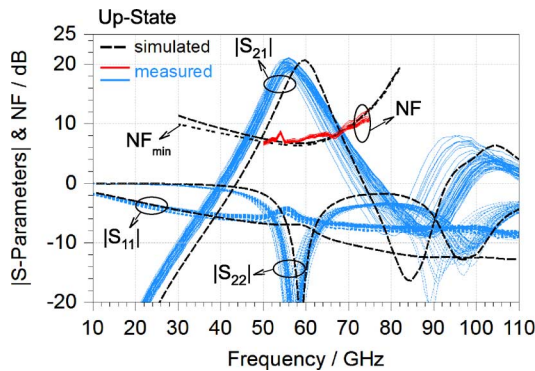


Fig. 6. Measured S-parameters and noise figure in comparison to the simulations for the up-state of the MEMS switches.

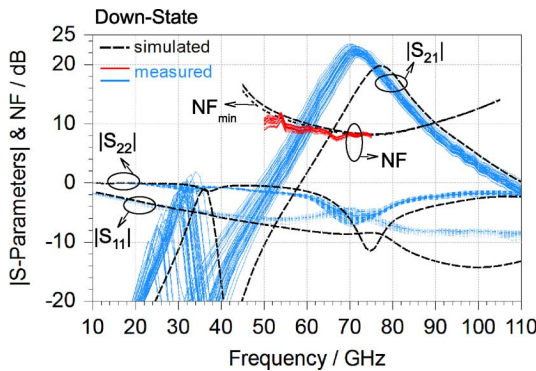


Fig. 7. Measured S-parameters and noise figure in comparison to the simulations for the down-state of the MEMS switches.

MEMS switches. The S-parameters measurements are performed over 50 samples on the same wafer, while 46 samples are displayed due to failed switch behavior in 4 samples. The NF measurements are performed only for a part of the processed wafer on 30 samples, while 27 samples are displayed in the figures. The peak gain of the measured samples are at around 56 GHz which is slightly below the targeted 60 GHz (6% lower), while the value of the gain is within the expected range. The $|S_{22}|$ measurements agree with the simulations, while $|S_{11}|$ values are around -5 dB, which is 3 dB worse than simulations. The measured NF is around 7 dB.

In Fig. 7, the measured S-parameters and NF of the designed 60/77 GHz switchable LNA are given for the down-state of the MEMS switches. For the down-state measurements, an actuation voltage of 40 V is applied. Similar to the up-state operation, the measured samples show a slight drop of frequency to around 72 GHz (6% lower). The gain is around 2 dB higher, $|S_{11}|$ is around -5 dB, 3 dB worse than the simulations, and $|S_{22}|$ varies from -7 to -5 dB, 3 to 5 dB worse than the simulated value. Because the frequency switching is achieved only by shortening of the load transmission lines, the $|S_{22}|$ perfor-

mance in the down-state is slightly worse than in the up-state. The measured NF is around 8 dB.

For both up- and down-states, the worst case $|S_{12}|$ equals -35 dB for the whole measurement range. The simulated $P_{1\text{dB}_{\text{in}}}$ equals -18 dBm for both states. In general, the measurements are in good agreement with the simulations, demonstrating the validity of the RF-MEMS switch models used in the designs. The slight deviations such as reduction in frequency or worse input/output matching are mainly associated with unaccounted parasitics, and lack of an accurate MIM-capacitor model.

The results are summarized in Table I, showing the minimum and maximum values of the measured gain and noise figure at 56 GHz for the up-state, and at 72 GHz for the down-state of the RF-MEMS switches. As seen, the designed switchable LNA achieves good performance in both bands, comparable to the state of the art in other BiCMOS technologies [5]–[7]. The switchable LNA outperforms conventional broadband designs, as in such designs more number of stages would be needed to maintain the high gain in both bands. These results verify the successful cofabrication of the RF-MEMS switches with the BiCMOS active devices, opening up many potential application possibilities in the millimeter wave frequency range.

V. CONCLUSION

Novel results of a 60/77 GHz switchable LNA in an RF-MEMS embedded 0.25 μm SiGe-C BiCMOS technology were presented. The measured samples showed good performance in both bands. The rather good agreement between measurement and simulation results, and the low spread across the wafer demonstrate that the presented technology is well suited for millimeter wave applications.

REFERENCES

- [1] G. Rebeiz, K. Entesari, I. Reines, S.-J. Park, M. El-tanani, A. Grichenner, and A. Brown, "Tuning in to RF MEMS," *IEEE Microw. Mag.*, vol. 10, no. 6, pp. 55–72, Oct. 2009.
- [2] G. Fedder, R. Howe, T.-J. K. Liu, and E. Quevy, "Technologies for cofabricating MEMS and electronics," *Proc. IEEE*, vol. 96, no. 2, pp. 306–322, Feb. 2008.
- [3] M. Kim, J. Hacker, R. Mihailovich, and J. DeNatale, "A monolithic MEMS switched dual-path power amplifier," *IEEE Microw. Componen. Lett.*, vol. 11, no. 7, pp. 285–286, Jul. 2001.
- [4] M. Kaynak, K. Ehwald, J. Drews, R. Scholz, F. Korndorfer, D. Knoll, B. Tillack, R. Barth, M. Birkholz, K. Schulz, Y. Sun, D. Wolansky, S. Leidich, S. Kurth, and Y. Gurbuz, "BEOL embedded RF-MEMS switch for mm-wave applications," in *Proc. IEEE Int. Electron Devices Meeting*, 2009, pp. 1–4.
- [5] V.-H. Do, V. Subramanian, and G. Boeck, "60 GHz SiGe LNA," in *Proc. Int. Conf. Electron., Circuits Syst.*, Marakesh, Morocco, Dec. 11–14, 2007, pp. 1209–1212.
- [6] A.-K. Chen, Y. Baeyens, Y.-K. Chen, and J. Lin, "A low-power linear SiGe BiCMOS low-noise amplifier for millimeter-wave active imaging," *IEEE Microw. Componen. Lett.*, vol. 20, no. 2, pp. 103–105, Feb. 2010.
- [7] B. Floyd, S. Reynolds, U. Pfeiffer, T. Zwick, T. Beukema, and B. Gaucher, "SiGe bipolar transceiver circuits operating at 60 GHz," *IEEE J. Solid-State Circuits*, vol. 40, no. 1, pp. 156–167, Jan. 2005.